Supplementary materials: A topological classification for intersection singularities of exceptional surfaces in pseudo-Hermitian systems

1. Pseudo-Hermiticity and metric operator

The pseudo-Hermiticity can be regarded as a symmetry in non-Hermitian physics [1], and a formal definition of pseudo-Hermiticity is always accompanied with a metric operator η

$$\eta H \eta^{-1} = H^{\dagger} \tag{S1}$$

Hence, a pseudo-Hermitian system is also called η-pseudo-Hermiticity, and the metric operator η is a Hermitian matrix. Recently, the parity-time inversion symmetry (*PT*) is included in pseudo-Hermiticity symmetry [2,3]. The considered system thus includes two inequivalent pseudo-Hermitian symmetries. In quantum mechanics, the Hamiltonians of two systems can be considered to be equivalent if they can transform to each other via unitary transformations ($U^{-1} = U^{\dagger}$)

$$H\varphi = E\varphi \rightarrow UHU^{\dagger}U\varphi = EU\varphi \rightarrow H'\varphi' = E\varphi' \tag{S2}$$

We apply the transformation to Eq. S1

$$\begin{aligned} & U\eta H\eta^{-1}U^{\dagger} = UH^{\dagger}U^{\dagger} \\ & \rightarrow U\eta U^{\dagger}UHU^{\dagger}U\eta^{-1}U^{\dagger} = UH^{\dagger}U^{\dagger} \\ & \rightarrow \eta' H' \eta'^{-1} = H'^{\dagger} \end{aligned} \tag{S3}$$

where $\eta' = U\eta U^{\dagger}$ is the transformed metric operator. One finds that the metric operator is not unique, and can transform with the Hamiltonian simultaneously. For the considered system in Eq. 2, one can apply an SU(2) rotation to the Hamiltonian, e.g.

$$\begin{aligned} & H' = e^{i\frac{\theta}{2}\sigma_1} H e^{-i\frac{\theta}{2}\sigma_1} \\ & = (f_2(\mathbf{k})i\sigma_2 + f_3(\mathbf{k})\sigma_3)\cos\theta + (-f_2(\mathbf{k})i\sigma_3 + f_3(\mathbf{k})\sigma_2)\sin\theta \end{aligned} \tag{S4}$$

It is found that the Hamiltonian can be transformed to a *PT* symmetric system with equal gain and loss for $\theta = \pi/2$,

$$H' = -f_2(\mathbf{k})i\sigma_3 + f_3(\mathbf{k})\sigma_2 \tag{S5}$$

and the metric operator is simultaneously transformed to

$$\eta' = \begin{bmatrix} 0 & i \\ -i & 0 \end{bmatrix} \tag{S6}$$

Hence, the classification in this work can be extended to other *PT* symmetric systems (e.g. realized by equal gain and loss, Eq. S5) [4].

2. Quotient space and stratified space

In topology, the quotient space of a topological space under given equivalent relations is a new topological space constructed by endowing the quotient set of the original topological space with the quotient topology [2]. Let (X, τ_X) be a topological space, and let ~ be equivalent relation on X. The

quotient set $Y=X/\sim$ is the set of equivalence classes of elements of X. The equivalence class of $x\in X$ is denoted by $[x]$. The quotient map associated with ~ refer to the surjective map

$$\begin{aligned} q: X &\to X/\sim \\ x &\to [x] \end{aligned} \tag{S7}$$

Intuitively speaking, any points of each equivalence class are identified or glued together. A well known example of quotient space is the Brillouin zone. In the momentum space of periodic systems, a point $\mathbf{k}$ is identified with points $\mathbf{k}+m_a\mathbf{G}_a$ because they have the same eigenvalues and eigenstates. Here $\mathbf{G}_a$ are reciprocal lattice vectors and m_a are integers. Besides, on the Brillouin zone boundaries, points under translations by $\mathbf{G}_a$ are also identified. Hence, there are two equivalent relations in the momentum space. As simple examples, the first Brillouin zone is a quotient map of the momentum space under equivalent relation of translations by $\mathbf{G}_a$, and point in the first Brillouin zone is an element in the equivalence class. For 1D periodic systems, identifying points on the Brillouin zone boundary constructs a quotient space, which is a 1D circle S^1 (see Fig. S1a1-a2). Similarly, the quotient space of the Brillouin zone of 2D periodic systems is a torus $S^1 \vee S^1$, which is a bouquet of two circles with a common base point (see Fig. S1b1-b3).

The momentum space of the considered system is a stratified space [6]. In topology, a stratified space is a triple (V,S,ζ), where V is a topological space (often we require it to be locally compact, Hausdorff, and second countable), S is a decomposition of V into strata $V=\bigcup_{X\in S} X$, and ζ is the set of control data $\{(T_X),(\pi_X),(\rho_X)|X\in S\}$, where T_X is an open neighborhood of the stratum X, π_X: $T_X\to X$ is a continuous retraction, and ρ_X: $T_X\to[0,+\infty)$ is a continuous function. These data need to satisfy the following conditions:

1. Each stratum T is a locally closed subset and the decomposition S is locally finite.

2. The decomposition S satisfies the axiom of the frontier: if $X, Y\in S$ and $T\in\bar{X}$. The condition implies that there is a partial order among strata: $Y<X$ if and only if $T\in\bar{X}$ and $Y\neq X$.

3. Each stratum is a smooth manifold.

4. $X=\{v\in T_X|\ \rho_X(v)=0\}$. So ρ_X can be viewed as the distance function from the stratum X.

5. For each pair of strata $Y<X$, the restriction (π_X, ρ_X): $T_X\bigcap X\to Y\times(0,+\infty)$ is a submersion.

6. For each pair of strata $Y<X$, there holds $\pi_Y\circ\pi_X=\pi_Y$ and $\rho_Y\circ\pi_X=\rho_Y$.

The exceptional surfaces and intersections in the considered system is a typical example. Here the decomposition S of V gives a set of strata X. The exceptional surfaces are hypersurfaces in momentum space and are singular varieties of X, and can be denoted by $Sing(X)$. The intersections of singular surfaces $Sing(Sing(X))$ eventually gives a natural stratification.

Our classification is based on eigenstates. The Hamiltonian in the real and imaginary line gaps can be expressed with the sum

$$H=\sum_{i=1,2} E_i \left|\varphi_i^L\right\rangle\left\langle\varphi_i^R\right| \tag{S8}$$

where $\varphi_i^{L(R)}$ denote the left and right eigenstates of the Hamiltonian. The pseudo-Hermiticity symmetry of the system enforces the left and right eigenstates to be connected by the following relation

$$\varphi_i^L = \eta \varphi_i^R \tag{S9}$$

The quotient space is constructed by identifying points with the same eigenstates. Hence, the construction from Fig. 1a-1b in the maintext can be easily understood, because antipodal points on ESs have the same eigenstates. In gaps, by adding a minus sign to the Hamiltonian in Eq. S8, the eigenenergies take negative signs, but the eigenstates remain the same. This process can be realized by taking the negatives of f_2 and f_3, which are just the antipodal points that lie in opposite regions with respect to the intersection. In our classification, the two points are identified because the sign change of eigenenergies does not matter. The constructed space Eq. (3) in the main text is a stratified quotient space, and the corresponding topology Eq. (4) is thus a quotient space topology.

3. Riemannian geometry in adiabatic transformations

The metric operator in pseudo-Hermiticity plays a similar role as the space-time metric in general relativity [7,8], and the eigenstates are like local coordinate frames (or tetrad). The local metric g can be defined with the indefinite inner product $g_{mn} = \langle \varphi_m \,|\, \eta \varphi_n \rangle$. The pseudo-Hermitian symmetry provides an orthogonality relation to eigenstates

$$\varphi_m^T \eta \varphi_n \begin{cases} = 0 & m \neq n \\ \neq 0 & m = n \end{cases} \tag{S10}$$

Since the Hamiltonian is gauged to be real, the eigenstates are real by removing arbitrary phases in exact phases ($|f_3|>|f_2|$), and thus the eigenstates have another orthogonal relation

$$\langle \varphi_m \,|\, \eta \varphi_n \rangle \begin{cases} = 0 & m \neq n \\ \neq 0 & m = n \end{cases} \tag{S11}$$

However, the self-inner products of the two eigenstates have opposite signs, i.e. one vector is space-like and the other is time-like, which imposes the Riemannian geometry of adiabatic transformations. In the following we will construct the relation between the adiabatic transformation and Lorentz boost i.e. SO(1,1) transformation.

Here we use the normalization $\varphi_m / \langle \varphi_m \,|\, \eta \varphi_m \rangle$ in exact phases, e.g. region I in Fig. 1a of the maintext, and the local metric can be obtained as

$$g = \begin{bmatrix} -1 & 0 \\ 0 & 1 \end{bmatrix} \tag{S12}$$

The dynamical problem is governed by

$$H \,|\varphi_m\rangle = i \partial_t \,|\varphi_m\rangle \tag{S13}$$

and completeness of eigenstates shows that a field can be expanded as

$$\phi_n(\lambda(t)) = \sum_m [U(\lambda(t))]^{-1}{}_n{}^m \varphi_m(\lambda(t)) \tag{S14}$$

Applying the partial derivative with respect to t, one obtains

$$
\begin{aligned}
i\frac{\partial}{\partial t}\phi_n(\lambda(t)) &= H[U(\lambda(t))]^{-1}{}_n{}^m \varphi_m(\lambda(t)) \\
&= i\frac{\partial[U(\lambda(t))]^{-1}{}_n{}^m}{\partial t}\varphi_m(\lambda(t)) + i[U(\lambda(t))]^{-1}{}_n{}^m \frac{\partial\varphi_m(\lambda(t))}{\partial t}
\end{aligned}
\tag{S15}
$$

The adiabatic approximation allows the instantaneous eigenvalue problem

$$
H(\lambda(t))\varphi_m(\lambda(t)) = E_m\varphi_m(\lambda(t)) \tag{S16}
$$

and applying a scalar product $\langle\varphi_l|$ from the left of Eq. S15 yields

$$
-iE_l[U(\lambda(t))]^{-1}{}_n{}^l = \frac{\partial[U(\lambda(t))]^{-1}{}_n{}^l}{\partial t} + \langle\varphi_l|\eta\frac{\partial|\varphi_m(\lambda(t))\rangle}{\partial t}[U(\lambda(t))]^{-1}{}_n{}^m \tag{S17}
$$

The partial derivative with respect to *t* can be expanded as

$$
\frac{\partial|\varphi_m(\lambda(t))\rangle}{\partial t} = \sum_k \frac{\partial|\varphi_m(\lambda(t))\rangle}{\partial\lambda^k}\frac{\partial\lambda^k}{\partial t} \tag{S18}
$$

We define the affine connection

$$
A_k{}^n{}_m = -\langle\varphi_n|\eta\frac{\partial|\varphi_m(\lambda(t))\rangle}{\partial\lambda^k} = -\langle\varphi_n|\eta\frac{\partial}{\partial\lambda^k}|\varphi_m\rangle \tag{S19}
$$

and the solution for U^{-1} is thus obtained as

$$
U^{-1} = \exp[\int_0^t ds\frac{\partial\lambda^k}{\partial s}A_k - i\int_0^t ds\omega(\lambda(s))] = \exp(\int_{\lambda(0)}^{\lambda(t)} d\lambda^k A_k)\times\exp[i\int_0^t dsE(\lambda(s))] \tag{S20}
$$

Ignoring the dynamical phase (the second term in Eq. S20), the geometric phase is simply

$$
U^{-1} = \exp(\int_{\lambda(0)}^{\lambda(t)} d\lambda^k A_k) \tag{S21}
$$

We would like to construct a relation between the affine connection and the local metric *g*. The local metric is a constant, and thus the partial derivative with respect to time is zero

$$
0 = \partial_t g_{mn} = \partial_t\langle\varphi_m|\eta\varphi_n\rangle \tag{S22}
$$

We insert the identity operator $I = \sum_l \eta|\varphi_l\rangle\langle\varphi_l|$ (obtained by Eq. S9) into Eq. S22

$$
\partial_{\lambda_k}\langle\varphi_m|\eta\varphi_n\rangle = \sum_l\langle\partial_{\lambda_k}\varphi_m|\eta|\varphi_l\rangle\langle\varphi_l|\eta\varphi_n\rangle + \sum_l\langle\varphi_m|\eta|\varphi_l\rangle\langle\varphi_l|\eta\partial_{\lambda_k}\varphi_n\rangle \tag{S23}
$$

One notes that

$$
\langle\partial_{\lambda_k}\varphi_m|\eta|\varphi_l\rangle = \langle\varphi_l|\eta|\partial_{\lambda_k}\varphi_m\rangle^* \tag{S24}
$$

and thus Eq. S23 can be written as

$$
0 = A_k^{*l}{}_m g_{ln} + g_{ml}A_k{}^l{}_n \tag{S25}
$$

Here the repeated index l means summed over according to the Einstein's summation rule [7]. The form of the metric Eq. S12 enforces the affine connection to have the following generators

$$T_1 = \begin{bmatrix} 0 & 1 \\ 1 & 0 \end{bmatrix}, \; T_2 = \begin{bmatrix} 0 & i \\ -i & 0 \end{bmatrix} \tag{S26}$$

The latter in Eq. S26 can be eliminated because the eigenstates are gauged to be real, and the former generator survives. It is shown that the adiabatic transformation of eigenstates is defined on the Lorentz group in 1+1 space-time, i.e. SO(1,1) group, revealing the Riemannian geometry of the adiabatic transformation. In broken phases, the transformation is also SO(1,1), and can be demonstrated with similar derivation processes. If we asign U(1) phases to the eigenstates $\varphi e^{i\psi}$ (ψ is constant), the Lorentz transformation becomes complex and the generator becomes a linear combination of $T_{1,2}$ in Eq. 26

$$T' = \begin{bmatrix} 0 & e^{i\chi} \\ e^{-i\chi} & 0 \end{bmatrix} \tag{S27}$$

which is still SO(1,1) transformation. Note that χ is a constant.

The Riemannian geometry of adiabatic transformation of eigenstates is very important in understanding the spin rotation of eigenstates and the presence of ESs. Taking T_1 in Eq. S26 as an example, the geometric phase induces a transformation

$$[\varphi_1', \varphi_2'] = [\varphi_1, \varphi_2] U^{-1} \tag{S28}$$

where U^{-1} is the transformation operator given by the geometric phase $U^{-1} = \exp \beta T_1$. As β approaches infinity $+\infty$, $\cosh\beta \approx \sinh\beta$, and thus

$$U^{-1} \to \mu \begin{bmatrix} 1 & 1 \\ 1 & 1 \end{bmatrix} \tag{S29}$$

As β approaches negative infinity $-\infty$, $\cosh\beta \approx -\sinh\beta$, and thus

$$U^{-1} \to \mu' \begin{bmatrix} 1 & -1 \\ -1 & 1 \end{bmatrix} \tag{S30}$$

where μ and μ' are real, which only induces the amplitude change of eigenstates without inducing spin rotations, and thus can be ignored. It is shown that eigenstates are parallel to each other as $\beta \to \pm\infty$, and as β varies from $(-\infty, +\infty)$, the final states are perpendicular to the initial states. Physical pictures of the spin rotations via adiabatic transformations have been given in Fig. 2 of the maintext.

4. Hybrid topological invariant of a closed loop circulating the CIL.

In the maintext, we showed that the invariant x (or y) and its inverse is sensitive to the sequence of eigenstates whenever the path (or loop) traverses the ESs. This is because the two eigenstates experience opposite geometric phases, and the sequence of the two eigenstates cannot be uniquely determined as the two bands (both eigenstates and eigenenergies) become degenerate at ESs. Hence, a close loop circulating the CIL has hybrid topological invariant. Hybrid topological invariant of intersection singularities was firstly discuss for exceptional point of order three (EP3) in [9]. The EP3 is a cusp intersection singularity, and its topological invariant is discussed in high dimensions. Here we do not attempt to extend the dimension with analytical continuation, because such process will break the symmetries (Eq. 1 in the maintext) of the system. Resultantly, the CIL is not expected to be present.

The CIL has 2^4=16 topological invariants as listed in Table 1, corresponding to different adiabatic variation processes of eigenenergies and eigenstates.

5. Composite invariants x^2 and y^2

In the maintext, we discussed the invariant x^2 on the loop in Fig. 3c. In the segmented path l_4, the sequence of the two eigenstates is changed, and thus the topology on l_4 is also x (instead of x^{-1}), the same as path l_2. Here we discuss another way to realize x^2. We firstly take a look at Fig. S2a, which is the quotient space constructed by the equivalent relation that antipodal points on ESs can be identified. Hence point A(B) can be identified with point A'(B'). As shown in Fig. S2(b1), the closed loop on the upper cone is a composite of the path l_1 (starts from A and terminates at B) and l_2 (starts from B' and terminates at A'). Under the convention given in the maintext, the invariants on both paths are also characterize by x, and hence the path A→B→B'→A' carries the invariant x^2. The corresponding adiabatic variation of eigenstates is shown in Fig. S2(b3), and the eigenstates experience $\mp\pi$ spin rotations ($\varphi'_{1,2} = \exp(\mp i\pi\sigma_2)\varphi_{1,2}$) with respect to y axis. The invariant y^2 can be realized in the same way (see Fig. S2b), which is a composite path C→D→D'→C', corresponding to the closed loop in the lower cone in Fig. S2a. The corresponding adiabatic variation process is shown in Fig. S3(b3)-(b4) (corresponding to real and imaginary parts of eigenstates). The eigenstates experience $\mp\pi$ spin rotations but a long z axis ($\varphi'_{1,2} = \exp(\mp i\pi\sigma_3)\varphi_{1,2}$).

Reference:

1. Mostafazadeh A. Pseudo-Hermitian representation of quantum mechanics[J]. International Journal of Geometric Methods in Modern Physics, 2010, 7(07): 1191-1306.
2. Zhang R, Qin H, Xiao J. PT-symmetry entails pseudo-Hermiticity regardless of diagonalizability[J]. Journal of Mathematical Physics, 2020, 61(1): 012101.
3. Mostafazadeh A. Pseudo-Hermiticity versus PT-symmetry III: Equivalence of pseudo-Hermiticity and the presence of antilinear symmetries[J]. Journal of Mathematical Physics, 2002, 43(8): 3944-3951.
4. Özdemir, Şahin Kaya, et al. "Parity–time symmetry and exceptional points in photonics." Nature materials 18.8 (2019): 783-798.
5. Spanier E H. Algebraic topology[M]. Springer Science & Business Media, 1989.
6. Ebeling, Wolfgang. The monodromy groups of isolated singularities of complete intersections. Vol. 1293. Springer, 2006.
7. Freedman D Z, Van Proeyen A. Supergravity[M]. Cambridge university press, 2012.
8. Frankel T. The geometry of physics: an introduction[M]. Cambridge university press, 2011.
9. Tang W, Jiang X, Ding K, et al. Exceptional nexus with a hybrid topological invariant[J]. Science, 2020, 370(6520): 1077-1080.

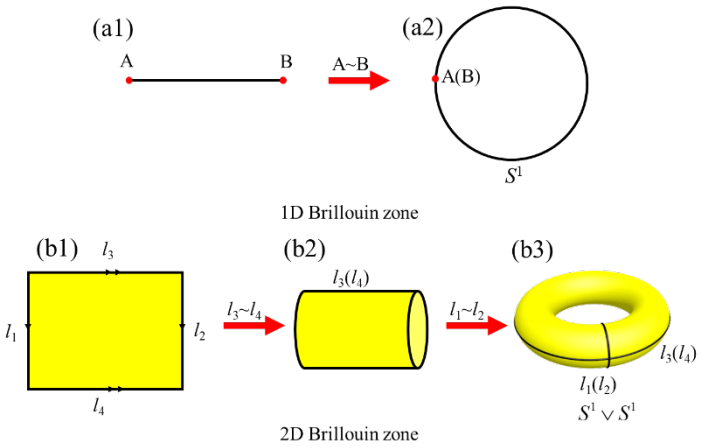

Fig. S1. Quotient space of momentum space in periodic systems. (a1)-(a2) The quotient space of 1D Brillouin zone is a circle (S^1) by identifying the two points on the Brillouin zone boundary. (b1)-(b3) Construction of quotient space of 2D Brillouin zone. Identifying the boundaries l_3 with l_4 gives a cylinder, which becomes a torus by identifying l_1 with l_2.

	$xyxy^{-1}$	$xyx^{-1}y$	$x^{-1}y^{-1}xy^{-1}$	$x^{-1}y^{-1}x^{-1}y$	
$xyx^{-1}y^{-1}$	$xy^{-1}x^{-1}y$	$x^{-1}yx^{-1}y$	$xy^{-1}xy^{-1}$	$x^{-1}yxy^{-1}$	$x^{-1}y^{-1}xy$
	$xy^{-1}x^{-1}y^{-1}$	$x^{-1}yx^{-1}y^{-1}$	$xy^{-1}xy$	$x^{-1}yxy$	
		$xyxy$	$x^{-1}y^{-1}x^{-1}y^{-1}$		

Table. S1. Hybrid topological invariant of a loop circulating the CIL. The invariants on the right hand side (with respect to the red line) are simply obtained by replacing the elements with their inverses.

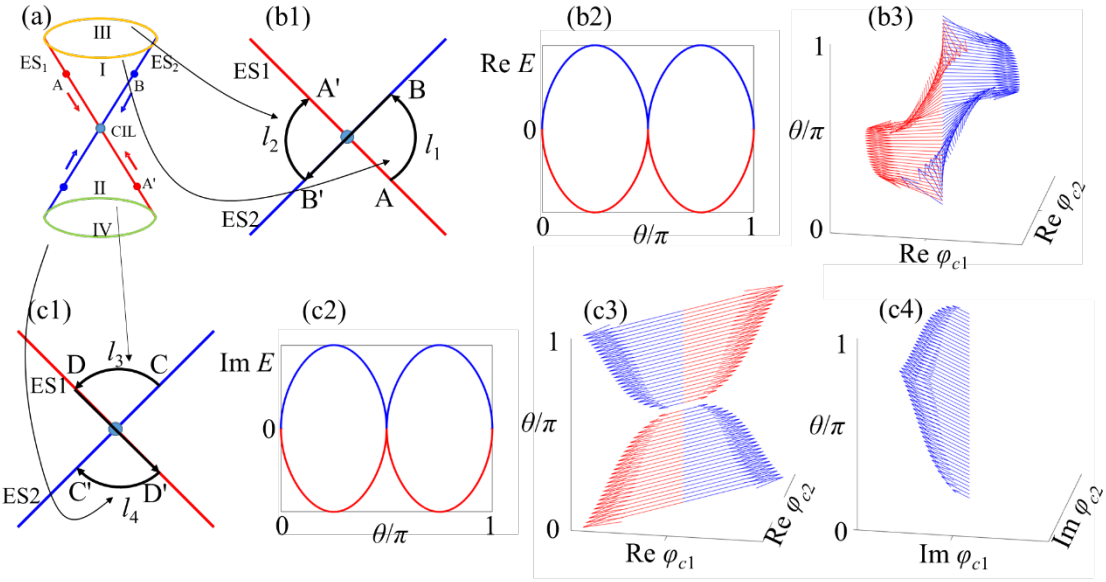

Fig. S2. Composite invariants x^2 and y^2. (a) The invariants corresponds to the loops in the double cone constructed by the first equivalent relation (identifying antipodal points on ESs). The closed loop in the upper and lower cone corresponds to the composite of paths l_1 and l_2 in (b1), and that of paths l_3 and l_4 in (c1), respectively. The corresponding adiabatic evolution of eigenvalues and eigenstates for x^2 is shown in (b2)-(b3), and those for y^2 are shown in (c2)-(c4).